

# Experimental characterization of semiconductor-based thermal neutron detectors

R. Bedogni<sup>a,\*</sup>, D. Bortot<sup>b,c</sup>, A. Pola<sup>b,c</sup>, M.V. Introini<sup>b,c</sup>, M. Lorenzoli<sup>b,c</sup>, J.M. Gómez-Ros<sup>a,d</sup>, D. Sacco<sup>a,e</sup>, A. Esposito<sup>a</sup>, A. Gentile<sup>a</sup>, B. Buonomo<sup>a</sup>, M. Palomba<sup>f</sup>, A. Grossi<sup>f</sup>

<sup>a</sup> INFN–LNF, via E. Fermi n. 40, 00044 Frascati, Roma, Italy

<sup>b</sup> Politecnico di Milano, Dipartimento di Energia, via La Masa 34, 20156 Milano, Italy

<sup>c</sup> INFN–Milano, Via Celoria 16, 20133 Milano, Italy

<sup>d</sup> CIEMAT, Av. Complutense 40, 28040 Madrid, Spain

<sup>e</sup> INAIL–DIT, Via di Fontana Candida 1, 00040 Monteporzio Catone, Italy

<sup>f</sup> ENEA Triga RC-1C.R. Casaccia, via Anguillarese 301, 00060 S. Maria di Galeria, Roma, Italy

## ARTICLE INFO

### Article history:

Received 7 November 2014

Received in revised form

13 January 2015

Accepted 15 January 2015

Available online 28 January 2015

### Keywords:

Thermal neutron detector

Neutron dosimetry

Neutron spectrometry

TRIGA

## ABSTRACT

In the framework of NESCOFI@BTF and NEURAPID projects, active thermal neutron detectors were manufactured by depositing appropriate thickness of  ${}^6\text{LiF}$  on commercially available windowless p–i–n diodes. Detectors with different radiator thickness, ranging from 5 to 62  $\mu\text{m}$ , were manufactured by evaporation-based deposition technique and exposed to known values of thermal neutron fluence in two thermal neutron facilities exhibiting different irradiation geometries. The following properties of the detector response were investigated and presented in this work: thickness dependence, impact of parasitic effects (photons and epithermal neutrons), linearity, isotropy, and radiation damage following exposure to large fluence (in the order of  $10^{12} \text{ cm}^{-2}$ ).

## 1. Introduction

The projects NESCOFI@BTF (2011–2013) and NEURAPID (2014–2016, <https://sites.google.com/site/csn5neurapid>) [1,2], supported by the Scientific Commission 5 of INFN (Italy), extensively investigated the possibility of developing real-time neutron spectrometers able to simultaneously cover all energy components of neutron fields, from thermal up to GeV. The final users of these instruments will be neutron-producing facilities, ranging from medical to industrial and research fields. The leading is to resume the functionality of the Bonner Sphere Spectrometer into a single moderator embedding multiple active thermal neutron detectors, with the important result of determining the complete spectrometric information in a single exposure constituents. The project proposed two different prototypal instruments [1], CYSP and SP<sup>2</sup>, exhibiting unidirectional or isotropic response, respectively. These spectrometers embed respectively seven or thirty-one internal thermal neutron detectors, thus the availability of low-cost thermal neutron detectors with adequate sensitivity, miniaturization, linearity and reproducibility was one of the most important project targets.

Commercially available thermal neutron detectors as  ${}^3\text{He}$  or  $\text{BF}_3$  counters were evaluated as basically unsuited, mainly due to the high cost. Diamonds covered with  ${}^6\text{LiF}$  [3] would be potentially good candidates, since their thermal neutron response per unit area is in principle the same as  ${}^6\text{LiF}$ -covered Silicon diodes. Nevertheless, monocrystalline diamonds are usually expensive and not available in the large area format required by the project. Poly-crystalline diamonds can be realized with quite large active areas, but their cost per unit area was still too high compared with the budget constraints of the project.

Satisfactory results were achieved with “in-house” detectors, obtained by depositing appropriate thickness of  ${}^6\text{LiF}$  powder on commercially available one  $\text{cm}^2$  windowless p–i–n diodes, with 0.3 mm nominal depletion layer. These are called TNPD (thermal neutron pulse detectors). TNPDs with different radiator thickness, ranging from 5 to 62 mm, were manufactured by evaporation-based deposition technique.

A standard analog chain formed by a charge preamplifier and a shaper amplifier was used to amplify the signal from the detectors. Detectors were used un-biased. A commercial digitizer (NI USB 6366), operating in streaming mode under a customized software written in LabView, allowed acquiring the data on a laptop. The spectrum elaboration was performed according to the procedure described in Ref. [4]. The detectors were exposed to known values

\* Corresponding author. Tel.: +39 0694032608.

E-mail address: [roberto.bedogni@lnf.infn.it](mailto:roberto.bedogni@lnf.infn.it) (R. Bedogni).

of thermal neutron fluence in two well-characterized thermal neutron facilities exhibiting different irradiation geometries:

- the ex-core radial column of the ENEA-Casaccia Triga reactor, exhibiting mono-directional distribution of the neutron fluence. The thermal beam normally impinged the detector surface. Different tests were performed, by operating the reactor at different power levels: 1, 10, 50 and 100 kW. The conventional thermal neutron fluence rate at the reference point in the thermal beam (hereafter called “thermal flux” to improve readability) was monitored every second through permanent monitor instruments (the so-called “linear amplifiers”). Accurate knowledge of the exposure time was possible through a pneumatic shutter, opening and closing the column in about one second. Previous measurements with gold foils made by TRIGA staff [5] allowed estimating in  $1420 \text{ cm}^{-2} \text{ s}^{-1} \text{ kW}^{-1}$  ( $\pm 5\%$  one s.d.) the reactor power to thermal flux conversion coefficient.
- the INFN-LNF thermal cavity obtained by moderating an Am-Be source with a polyethylene cylinder, with nearly isotropic distribution of the neutron fluence. Here the thermal flux at the point of test is  $1270 \text{ cm}^{-2} \text{ s}^{-1}$  ( $\pm 3\%$  one s.d.) and the direction distribution of the field is roughly isotropic [6].

The following aspects were studied and presented in this work:

- Understanding the role of the radiator and of the semiconductor itself in the thermal neutron response and the effect of epithermal neutrons on the response. This was achieved by exposing bare and deposited detectors in absence or presence of a 1 mm thick Cd absorber;
- Determining the detector response, in terms of thermal neutron counts per unit fluence ( $\text{cm}^2$ ), as a function of the radiator thickness;
- Response linearity;
- Response isotropy, evaluated by comparing the response in mono-directional and isotropic fields;
- Modification of the response following exposure to large thermal fluence (in the order of  $10^{12} \text{ cm}^{-2}$ ), or radiation damage due to thermal neutrons.

## 2. Understanding the detector response

Being formed by a Silicon diode coupled to a  $^6\text{LiF}$  radiator, the TNPD response to neutrons N, i.e. the pulse height distribution (PHD) of events interacting with the diode active volume, is generally given by superimposition of the following contributions:

$$N(V) = R_{\text{th}}(V) + R_{\text{epi}}(V) + S_{\text{th}}(V) + \gamma(V), \quad (1)$$

where  $V$  is the pulse height,  $R_{\text{th}}(V)$  is the PHD due to thermal neutrons (below 0.4 eV) interacting in the radiator,  $R_{\text{epi}}(V)$  is the PHD due to epi-thermal neutrons interacting in the radiator,  $S_{\text{th}}(V)$  is the PHD due to thermal neutrons interacting in the Silicon substrate, where some minimal amount of Boron may be present. In principle also the epithermal contribution  $S_{\text{epi}}$  should be accounted, but its contribution is expected to be completely negligible,  $\gamma(V)$  is the PHD due to secondary particles generated by photons accompanying the neutron field and interacting in the Silicon substrate.

The classical method to infer  $R_{\text{th}}(V)$  is to expose the TNPD with and without a 1 mm thick Cd absorber in the form of a box covering the whole detector. However, this introduces a further term  $\gamma_{\text{Cd}}(V)$ , i.e. the PHD due to prompt photons coming from the neutron capture in the Cadmium filter. To investigate these aspects, additional exposures were performed with a non-deposited detector (bare) with and without the 1 mm thick Cd box. The PHDs obtained in the four cases are described by Eq. (1)

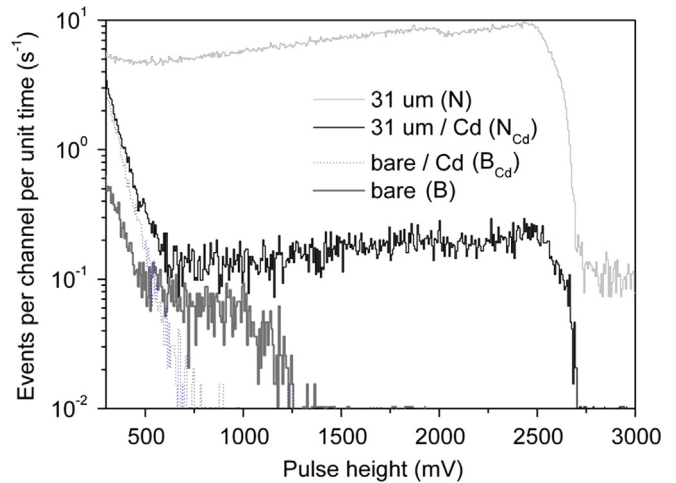


Fig. 1. Pulse height distributions for the 31  $\mu\text{m}$  TNPD and the bare detector exposed with and without the Cd box at 50 kW. Data are normalized to the unit time. Channel width = 3 mV.

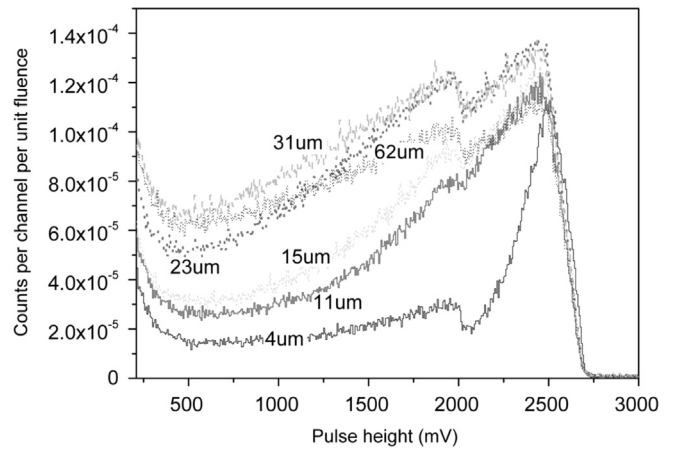


Fig. 2. Pulse height distribution  $N-N_{\text{Cd}}$  for the TNPD with different thickness exposed to the ex-core thermal field of the TRIGA reactor at power 50 kW. Data are normalized to the unit thermal fluence. Channel width = 3 mV.

plus the following:

$$N_{\text{Cd}}(V) = R_{\text{epi}}(V) + \gamma(V) + \gamma_{\text{Cd}}(V) \quad (2)$$

$$B(V) = S_{\text{th}}(V) + \gamma(V) \quad (3)$$

$$B_{\text{Cd}}(V) = \gamma(V) + \gamma_{\text{Cd}}(V) \quad (4)$$

where  $N_{\text{Cd}}(V)$ ,  $B(V)$  and  $B_{\text{Cd}}(V)$  are respectively the PHDs of the TNPD under Cd, of the bare silicon detector, and of the bare silicon detector under Cd.

By combining the equations, the term  $R_{\text{th}}(V)$  can be obtained by  $(N(V) - B(V) - (N_{\text{Cd}}(V) - B_{\text{Cd}}(V)))$ . The four spectra  $N(V)$ ,  $N_{\text{Cd}}(V)$ ,  $B(V)$  and  $B_{\text{Cd}}(V)$  are shown in Fig. 1 for the 31  $\mu\text{m}$  detector (highest response) in the TRIGA thermal beam at power 50 kW. Data are normalized to the unit exposure time. The  $N(V)$  spectrum shows a double-peaked structure (more evident in Fig. 2), given by the reaction products  $\alpha$  and  $T$ , having respectively energy 2.05 and 2.73 MeV and range in LiF 6  $\mu\text{m}$  and 30  $\mu\text{m}$ . The conversion coefficient from pulse height to deposited energy is roughly  $1 \text{ MeV V}^{-1}$ . This was determined by electronic calibration, using a pulse generator, and confirmed by the position of the alpha and triton peaks in the spectrum.

The residual neutron captures in the Cd-covered configuration ( $N_{\text{Cd}}$ ) are due to epithermal neutrons. The same spectrum also shows a photon contribution (region below 500 mV) arising from

the prompt gammas from neutron captures in Cd. This added gamma component (previously symbolized  $\gamma_{Cd}$ ) is more important than the contribution of the photons originally present in the field ( $\gamma$  in previous formalism). The presence of a small amount of boron in the semiconductor is proved by the disappearance of the events from 700 to 1500 mV when the bare detector is covered with Cd ( $B_{Cd}$ ). The end-point 1500 mV in the B spectrum corresponds to the energy of the  $\alpha$  particle from the  $^{10}B(n,\alpha)^7Li$  reaction. The photons, either coming from the external field or from the captures in Cd, only contribute in the region below about 500 mV. Thus, when determining an integral reading from a spectrum, a lower integration limit 600 mV is chosen to reduce photon sensitivity to the minimum extent. This integral is hereafter called “response”. When calculating the response for the spectra shown in Fig. 1, one obtains the following quantities (for simplicity, the symbols previously used for the PHDs are hereafter used for the corresponding integral responses):  $N=2330\text{ s}^{-1}$ ,  $N_{Cd}=56.5\text{ s}^{-1}$ ,  $B=6.0\text{ s}^{-1}$ ,  $B_{Cd}=0.90\text{ s}^{-1}$ . Therefore:

- the epithermal contribution to the detector reading ( $N_{Cd}/N$ ) is only 2.4%;
- the difference between  $(N-N_{Cd})$  and  $(N-B-N_{Cd}+B_{Cd})$  is only 0.2%, thus reducing the importance of exposing the bare detector with and without Cd in further measurements in this field.

It should be noted that these considerations are only valid for this specific field. For other fields, especially in cases where the photon or the epithermal neutron contributions are expected to be higher, this study should be repeated with all the four detector combinations.

### 3. Response and radiator thickness

Because one of the project objectives was depositing large numbers of detectors at the same time at basically no cost (other than the lithium fluoride), a simple evaporation technique was implemented. To achieve good deposit robustness, the lithium fluoride was mixed with small amounts of other compounds.

Repeated depositions with the same nominal amount  $^6LiF$  allowed estimating the accuracy of the deposited layer in about  $1\text{ }\mu\text{m}$  for thickness lower than  $10\text{ }\mu\text{m}$ , and 2 to  $3\text{ }\mu\text{m}$  above. Detectors were manufactured with the following thickness ( $t$ ) values:  $4\text{ }\mu\text{m}$ ,  $11\text{ }\mu\text{m}$ ,  $15\text{ }\mu\text{m}$ ,  $23\text{ }\mu\text{m}$ ,  $31\text{ }\mu\text{m}$  and  $62\text{ }\mu\text{m}$ . The  $N-N_{Cd}$  spectra obtained after exposure in the TRIGA reactor at 50 kW are shown in Fig. 2 for all detectors. The tritium peak in the  $4\text{ }\mu\text{m}$  spectrum is so narrow because the tritium range (about  $30\text{ }\mu\text{m}$ ) is considerably higher than  $t$ , thus the attenuation effect in the radiator is very limited. By contrast, the alpha peak is more broadened because the alpha range is similar to  $t$ . This difference becomes gradually less important when increasing the value of  $t$ . The maximum response ( $t=31\text{ }\mu\text{m}$ ) is achieved when  $t$  equals the range of tritium, corresponding to the “build-up” condition for the reaction products. For greater thicknesses ( $62\text{ }\mu\text{m}$ ) the self-absorption of thermal neutrons becomes important and the detector response decreases. The dependence of the integral response from the radiator thickness is more clearly shown in Fig. 4.

### 4. Response linearity

The linearity of the TNPd response was evaluated by considering exposures in the TRIGA reactor at power levels 1, 10, 50 and 100 kW, corresponding in thermal fluence rate to about  $1.7E+3$ ,  $1.7E+4$ ,  $7.9E+4$  and  $1.7E+5\text{ cm}^{-2}\text{ s}^{-1}$ . The data in terms of “pure thermal” response ( $N-N_{Cd}$ ) are graphically shown in Fig. 3. The effect of adding the term  $B_{Cd}$  is always in the order of 0.1% or lower, so it can be neglected for practical purposes. The response vs reactor power

relation is linear, thus the best estimation of the thermal response per unit fluence was obtained by fitting the plots, see Table 1 (second column). Here uncertainties ranges from 6% to 8%, coming from combining the fitting uncertainty (4% to 6%, coming from reproducibility of power monitoring) with the power-to-thermal flux conversion coefficient (5%). As anticipated in Section 2, the response monotonically increases with the thickness up to  $31\text{ }\mu\text{m}$ . Again, the impact of the thermal neutron self-absorption is evident in the  $62\text{ }\mu\text{m}$  detector. Column 2 of Table 1 is plotted in Fig. 4.

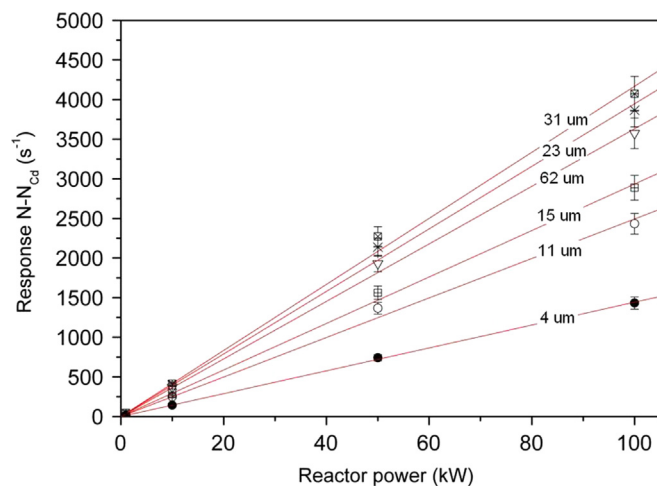


Fig. 3. Linearity plot for different detector thickness achieved with reactor power 1, 10, 50 and 100 kW.

Table 1

Response per unit thermal fluence for different values of detector thickness.

Thickness ( $\mu\text{m}$ )	Response per unit fluence $(N-N_{Cd})/\phi$ ( $10^{-2}\text{ cm}^2$ )	
	TRIGA (fitted response)	$^{241}\text{Am-Be}$ moderated field
4	$1.02 \pm 0.07$	$1.00 \pm 0.04$
11	$1.76 \pm 0.14$	$1.81 \pm 0.07$
15	$2.07 \pm 0.13$	$2.04 \pm 0.07$
23	$2.78 \pm 0.20$	$2.68 \pm 0.10$
31	$2.94 \pm 0.23$	$2.95 \pm 0.11$
62	$2.56 \pm 0.16$	$2.70 \pm 0.10$

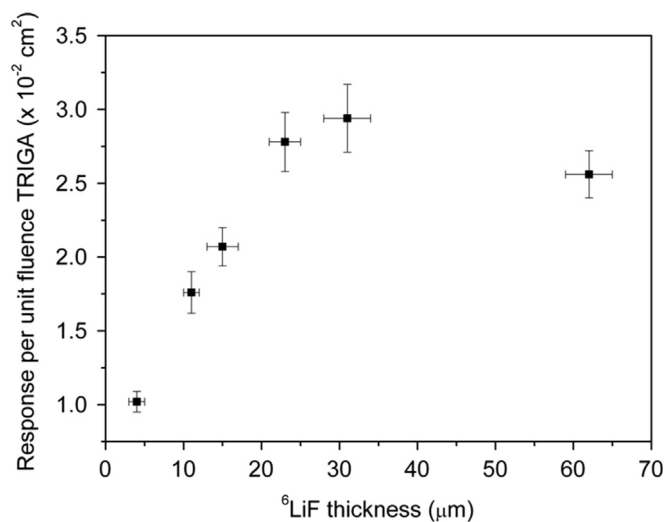


Fig. 4. Dependence of the integral response ( $N-N_{Cd}$ ) from the radiator thickness.

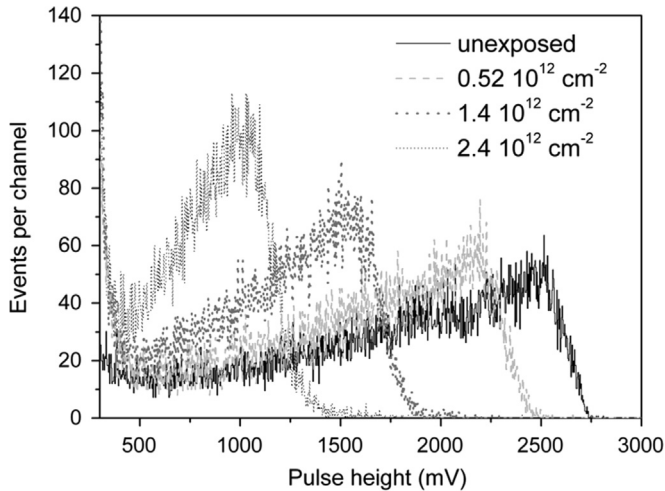


Fig. 5. Effect of high flux thermal neutron irradiation on the spectrum from the 15  $\mu\text{m}$  TNPd. The term “unexposed” means before introducing the detector in the reactor core. In legend the accumulated thermal fluence is reported. The spectra correspond to a constant value of thermal fluence of  $8.5 \times 10^5 \text{ cm}^{-2}$ .

### 5. Effect of changing the direction distribution of the thermal field

A preliminary evaluation of the angle response of the TNPd was performed by comparing the data obtained in the TRIGA thermal beam (mono-directional) with those obtained in the INFN-LNF  $^{241}\text{Am}$ -Be moderated field, considered as roughly isotropic [6], see Table 1 (Column 3). The epithermal contribution to the detector reading  $N_{\text{Cd}}/N$  is, in the case of the  $^{241}\text{Am}$ -Be moderated field, about 1.6%.

For the fields considered in this study, the differences in direction distribution of the fluence do not result in different detector responses. However, a further measurement campaign at the TRIGA thermal beam, using a rotating holder, is planned to investigate the response at large incidence angles between the neutron direction and the detector surface.

### 6. Detector damage induced by irradiation to large fluence

Because one of the final applications of the TNPds is to be embedded in moderator-based beam monitors, quantifying the radiation-induced damage was an important task. A 15  $\mu\text{m}$  detector was tested after exposure to large values of thermal fluence (in the order of  $10^{12} \text{ cm}^{-2}$ ). This was achieved by positioning the detector in the reactor core, through a “rabbit” motion system, for fixed time intervals. The reactor was operated at 1 kW. After every irradiation interval (in the order of 100 s), the detector was tested in the ex-core facility at the same power level and the PHD was recorded. The results are shown in Fig. 5. Large exposures affect the reticular structure of the Silicon, thus resulting in altered charge collection properties. The spectrum is shifted on the left,

and the double peaked structure tends to contract in a single peak. This shift, evaluated at the end point of the distribution, may be quantified in about  $-30\%$  per  $10^{12} \text{ cm}^{-2}$ . By contrast, the integral response is only slightly affected ( $-5\%$  per  $10^{12} \text{ cm}^{-2}$ ).

### 7. Conclusions

In order to equip the single-moderator multi-detector prototypes CYSP and SP<sup>2</sup> designed in the NESCOFI@BTF and NEURAPID projects, low-cost thermal neutron detectors were manufactured by depositing thin layers of  $^6\text{LiF}$  (from 4 to 62  $\mu\text{m}$ ) on commercially available  $1\text{-cm}^2$  windowless p-i-n diodes. The deposition was performed with an inexpensive evaporation-based method, suitable for large-scale production. Data from the detectors were acquired through a customized Labview-based DAQ system. Their responses were studied in thermal fields with different intensity and direction distribution, produced in the ex-core radial column of the ENEA-Casaccia Triga reactor (mono-directional, with thermal flux varying from  $10^3$  up to  $10^5 \text{ cm}^{-2}\text{s}^{-1}$ ) or in the INFN-LNF  $^{241}\text{Am}$ -Be moderated field (roughly isotropic, thermal flux  $1.3 \times 10^3 \text{ cm}^{-2} \text{ s}^{-1}$ ). The parasitic effects of epithermal neutrons or photons on the detector response were studied using bare and deposited detectors in absence or presence of a 1 mm thick Cd absorber. The response as a function of the radiator thickness was investigated. In addition, response linearity, isotropy and radiation damage were assessed. The satisfactory results of these tests, together with the small dimension and the low cost (considerably lower than any other commercially available sensor with comparable sensibility) qualify these detectors as suitable for the active versions of the CYSP and SP<sup>2</sup> to be employed in a large variety of low- and medium-intensity neutron fields. To measure high fluence rates (higher than  $10^9 \text{ cm}^{-2} \text{ s}^{-1}$ ), the same  $^6\text{LiF}$  deposition technique could be employed on more radiation-resistant semiconductors, as SiC.

### Acknowledgements

This work has been supported by the INFN projects NESCOFI@BTF and NEURAPID (Commissione Scientifica Nazionale 5).

### References

- [1] R. Bedogni, J.M. Gómez-Ros, D. Bortot, A. Pola, M.V. Introini, A. Esposito, A. Gentile, G. Mazzitelli, B. Buonomo, *Radiation Protection Dosimetry* 161 (2014) 37.
- [2] A. Pola, D. Bortot, M.V. Introini, R. Bedogni, A. Gentile, A. Esposito, J.M. Gómez-Ros, E. Passoth, A. Prokofiev, *Radiation Protection Dosimetry* 161 (2014) 229.
- [3] M. Angelone, G. Aielli, S. Almaviva, R. Cardarelli, D. Lattanzi, M. Marinelli, E. Milani, G. Prestopino, M. Pillon, R. Santonico, A. Tucciarone, C. Verona, G. Verona-Rinati, *IEEE Transactions on Nuclear Science* NS56 (2009) 2275.
- [4] R. Bedogni, D. Bortot, B. Buonomo, A. Esposito, J.M. Gómez-Ros, M.V. Introini, M. Lorenzoli, A. Pola, D. Sacco, *Nuclear Instruments and Methods in Physics Research Section A* 767 (2014) 159.
- [5] A. Grossi, Private Communication, 2012.
- [6] R. Bedogni, D. Bortot, A. Pola, M.V. Introini, A. Gentile, A. Esposito, J.M. Gómez-Ros, M. Palomba, A. Grossi, *Radiation Protection Dosimetry* 161 (2014) 241.